

# Low-Band-Gap Conjugated Polymers Based on Thiophene, Benzothiadiazole, and Benzobis(thiadiazole)

Eva Bundgaard and Frederik C. Krebs\*

The Danish Polymer Centre, RISØ National Laboratory, P.O. Box 49, DK-4000 Roskilde, Denmark

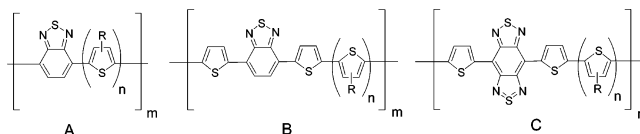
Received December 15, 2005; Revised Manuscript Received February 13, 2006

**ABSTRACT:** A series of low-band-gap copolymers of thiophene, benzothiadiazole, and benzobis(thiadiazole) were synthesized. The polymers were synthesized by Stille cross-coupling polymerization of distannylalkylthiophenes and dithiophenes with dibromo derivatives of benzothiadiazoles and benzobis(thiadiazole)s. The polymers were characterized using NMR, UV–vis, and size exclusion chromatography (SEC). The molecular weight, solubility, and film-forming ability were highly dependent on the choice of side chains. 3,7,11-Trimethyldodecyl side chains were found to give polymer products with high molecular weight, good film-forming ability, and good solubility. Band gaps were estimated from UV–vis to be 2.1–1.7 eV for polymers based on benzothiadiazole and ~0.7 eV for polymers based on benzobis(thiadiazole). The band gap and electronic structure of the polymers were determined by a combination of UV–vis spectroscopy and ultraviolet photoelectron spectroscopy (UPS).

## Introduction

Polymer photovoltaics<sup>1</sup> bring promise as a future renewable source of energy, and while a few difficult problems need to be solved before commercialization of polymer photovoltaics for electrical energy production becomes a reality, the hopes are high. Intensive research has already led to a technology that is suitable for low-energy niche applications. The cost and environmental benefits using this technology are attractive, and the problems remain with the lifetime and the efficiency of experimental devices. While recent improvements of both efficiency<sup>1i</sup> and lifetime<sup>1h</sup> have been reported, further improvements are desirable. In terms of efficiency, many factors influence the relatively low efficiencies of around 5% that has been reported. In particular, the conjugated polymers that are typically employed as the active material exhibit a poor overlap with the solar spectrum. The band gaps are typically higher than 2.0 eV, and it is believed that lower band gaps could increase the efficiency by harvesting a larger proportion of the sunlight. There are limits to how low a band gap one can apply as the exciton binding energy becomes significant at lower energies, and while a too low band gap will result in harvesting of more photons with lower energy, excessive loss will ensue and lead yet to poorer efficiencies. Because of the unavailability of conjugated polymer materials with low band gaps, there have been few reports on the use of low-band-gap conjugated polymer materials in polymer photovoltaic devices, and therefore experimental evidence on the applicability remains scarce. For this reason low-band-gap polymers have received considerable attention recently.<sup>2–5</sup> Spectral coverage in the range from 700 to 1200 nm (1.8 to 1 eV, respectively) is believed to enable the fabrication of photovoltaic devices with increased conversion efficiency.<sup>2,3</sup> From a synthetic point of view low-band-gap conjugated materials are however a challenge, and only a few families of polymers exist. The most important ones have been polyisothianaphthenes,<sup>6,7</sup> polythiophenes,<sup>1,8,9</sup> and copolymers of benzothiadiazole, thiophene, and pyrrole.<sup>3–5</sup> Generally, low-band-gap materials have been problematic in terms of solubility, and for this reason the preparation of soluble materials was paramount in this work.

**Chart 1.** R = 3,7,11-Trimethyldodecyl for (A)  $n = 1, 2$ , for (B)  $n = 1, 2$ , and for (C)  $n = 1, 2$ ; R = 2-Ethylhexyl for (B)  $n = 2$



In this paper, we describe the synthesis and characterization of soluble low-band-gap copolymers of thiophenes with benzothiadiazole and benzobis(thiadiazole)s of the types shown in Chart 1. Syntheses were carried out by oxidative ferric chloride polymerization and Stille cross-coupling polymerization.

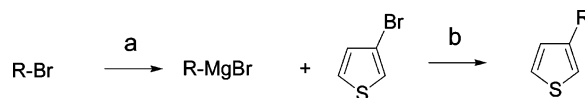
## Results and Discussion

Monomers for Stille cross-coupling polymerization were distannyl derivatives of 3-(3,7,11-trimethyldodecyl)thiophene or di(3,7,11-trimethyldodecyl)dithiophene and dibromo derivatives of benzothiadiazole or benzobis(thiadiazole). For the oxidative ferric chloride polymerization, di(2-ethylhexyl)dithiophene–benzothiadiazole was used.

**Synthesis of Monomers.** The synthesis of the long and branched alkyl chain 3,7,11-trimethyldodecyl bromide was carried out as described in the literature.<sup>10</sup> The reported hydrogenation of farnesol to give 3,7,11-trimethyldodecanol was modified using high contents of Pd/C 10 wt % (0.2 mol % Pd) instead of Adams catalyst (PtO<sub>2</sub>) and a pressure at 45 bar. In the paper by Schouten et al.<sup>10</sup> the temperature and pressure were not reported, and our initial attempts were carried out at 4 bar. This gave only a partially hydrogenated product, and we found that large amounts of 10% Pd/C at 45 bar and 60 °C were required to complete the reaction in 1 day.

Addition of 3,7,11-trimethyldodecylmagnesium bromide to 3-bromothiophene to give 3-(3,7,11-trimethyldodecyl)thiophene (**1**) was carried out by a Kumada reaction (Scheme 1).<sup>11</sup> Even

**Scheme 1.** Synthesis of Alkylthiophene<sup>a</sup>



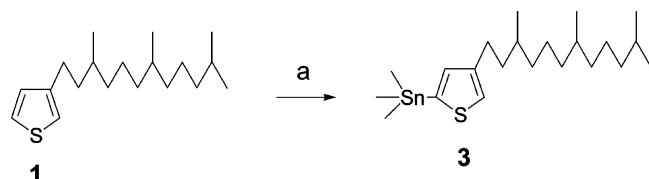
<sup>a</sup> a: Mg, ether; b: Nidppp, R = 3,7,11-trimethyldodecyl (**1**) and 2-ethylhexyl (**2**).

though the bromoalkane was added slowly and dropwise to the magnesium turnings during the Grignard reaction, a small amount of the Wurtz coupled byproduct, 2,6,10,15,19,23-hexamethyltetracosane, was formed. After purification, the final product contained around 7% of 2,6,10,15,19,23-hexamethyltetracosane. This byproduct was found difficult to remove and was alleviated in later reaction steps.

The synthesis of 3-(2-ethylhexyl)thiophene (**2**) was also carried out by Kumada reaction (Scheme 1).<sup>11</sup>

**Lithiation of 3-Alkylthiophene.** Compound **1** was lithiated with *n*BuLi and TMEDA followed by reaction with trimethylstannyl chloride to give 4-(3,7,11-trimethyldodecyl)-2-trimethylstannylthiophene (**3**) (Scheme 2).

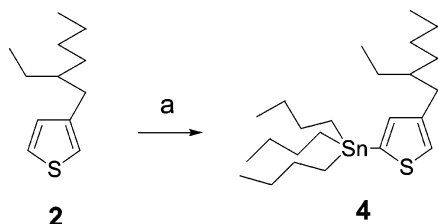
Scheme 2. Lithiation of **1** with *n*BuLi<sup>a</sup>



<sup>a</sup> a: (1) *n*BuLi, TMEDA, hexane,  $-78^{\circ}\text{C}$ ; (2)  $\text{Me}_3\text{SnCl}$ ,  $-78^{\circ}\text{C}$ .

The reaction with *n*BuLi and TMEDA (1.5 equiv) resulted in modest yields of the product (54%). Compound **2** was lithiated with LDA<sup>12</sup> and reacted with tributylstannyl chloride to give 4-(2-ethylhexyl)-2-tributylstannylthiophene (**4**) (Scheme 3). The reaction with LDA resulted in a mixture of starting material and product, and hence the yield was lower (42%) compared to the lithiation using *n*BuLi and TMEDA.

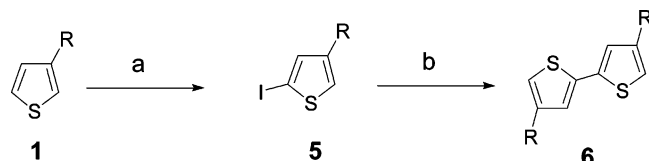
Scheme 3. Lithiation of **2** with LDA<sup>a</sup>



<sup>a</sup> a: (1) LDA, THF,  $-78^{\circ}\text{C}$ ; (2)  $\text{Bu}_3\text{SnCl}$ ,  $-78^{\circ}\text{C}$ .

**Dithiophene.** The synthesis of 4,4'-bis(3,7,11-trimethyldodecyl)-2,2'-dithiophene (**6**) was carried out by Stille coupling between **3** and 2-iodo-4-(3,7,11-trimethyldodecyl)thiophene (**5**) to give the tail-to-tail product **6** (Scheme 4). Compound **5** was made in one-pot by addition of  $\text{I}_2$  to **3** and was not isolated before performing the Stille coupling under reflux. This reaction resulted in a pure tail-to-tail product **6**. We ascribe this to a faster reaction between **3** and **5** compared to reaction between the 2-bromo-3-(3,7,11-trimethyldodecyl)thiophene (**7**) and **3**. In **3** and **5** there is least sterical hindrance where **7** exhibits more sterical hindrance due to the alkyl group adjacent to bromine. Hence, no homocoupling of **3** was observed, and further, decomposition of **3** to **1** was not observed.

Scheme 4. Synthesis of **6**, R = 3,7,11-Trimethyldodecyl<sup>a</sup>



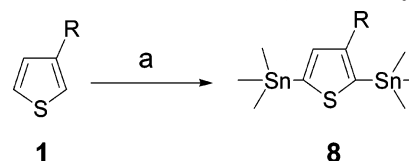
<sup>a</sup> a: (1) *n*BuLi, THF,  $-78^{\circ}\text{C}$ ; (2)  $\text{I}_2$ ; (b) **3**,  $\text{Pd}(\text{PPh}_3)_2\text{Cl}_2$ , reflux.

Several other attempts were made to synthesize head-to-head and head-to-tail isomers of **6**; these are described in the Supporting Information.

The large-scale synthesis of 3,4'-dihexyl-2,2'-dithiophene has been described in the literature.<sup>12</sup> The reaction between 2-bromo-3-hexylthiophene and 4-hexyl-2-trimethylstannylthiophene resulted in three isomers of the product. The purification of this mixture was complicated,<sup>12</sup> and synthesis of only one isomer is preferred.

**Dilithiation of 3-Alkylthiophenes.** The dilithiation of **1** was carried out using 5 equiv of *t*BuLi. This reaction resulted in dilithiation after  $3\frac{1}{2}$  days at room temperature. Addition of trimethylstannyl chloride gave the product 3-(3,7,11-trimethyldodecyl)-2,5-bis(trimethylstannyl)thiophene (**8**) (Scheme 5). Other attempts were made to dilithate **1** (see Supporting Information).

Scheme 5. Dilithiation of **1**, R = 3,7,11-Trimethyldodecyl<sup>a</sup>

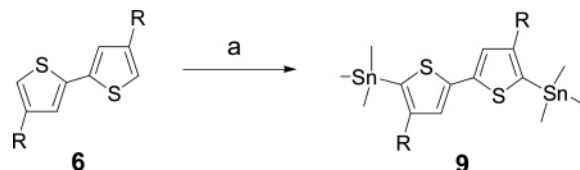


<sup>a</sup> a: (1) *t*BuLi, hexane, RT; (2)  $\text{Me}_3\text{SnCl}$ ,  $-78^{\circ}\text{C}$ .

These results show that the dilithiation of 3-alkylthiophenes requires a stronger base than the monolithiation. This is ascribed to a lower acidity of the protons in alkylthiophene monoanions.

**Dilithiation of Dialkylthiophene.** The dilithiation of **6** was successfully carried out using *n*BuLi and TMEDA (3 equiv) which resulted in dilithiation after 1 h, and addition of trimethylstannyl chloride gave the product 4,4'-bis(3,7,11-trimethyldodecyl)-5,5'-bis(trimethylstannyl)-2,2'-dithiophene (**9**) (Scheme 6). Other attempts were made to dilithate **6** (see Supporting Information).

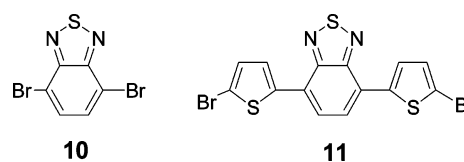
Scheme 6. Dilithiation of **6**, R = 3,7,11-Trimethyldodecyl<sup>a</sup>



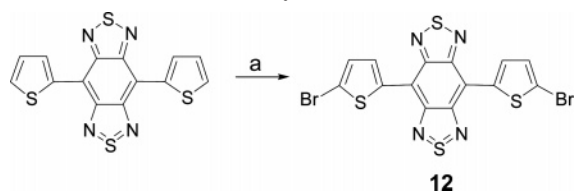
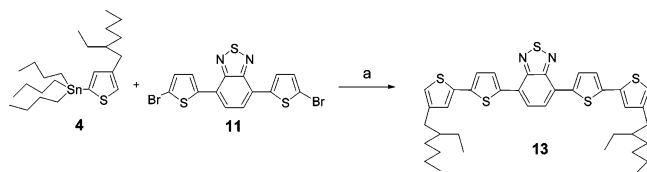
<sup>a</sup> a: (1) *n*BuLi, TMEDA, hexane,  $-78^{\circ}\text{C}$ ; (2)  $\text{Me}_3\text{SnCl}$ ,  $-78^{\circ}\text{C}$ .

**Dibromo Derivatives of Benzothiadiazole and Benzobis(thiadiazole).** The synthesis of both 4,7-dibromobenzo-[2,1,3]-thiadiazole (**10**) and 4,7-di(5-bromothiophen-2-yl)benzo-[2,1,3]-thiadiazole (**11**) have been described in the literature (Scheme 7).<sup>13,14</sup>

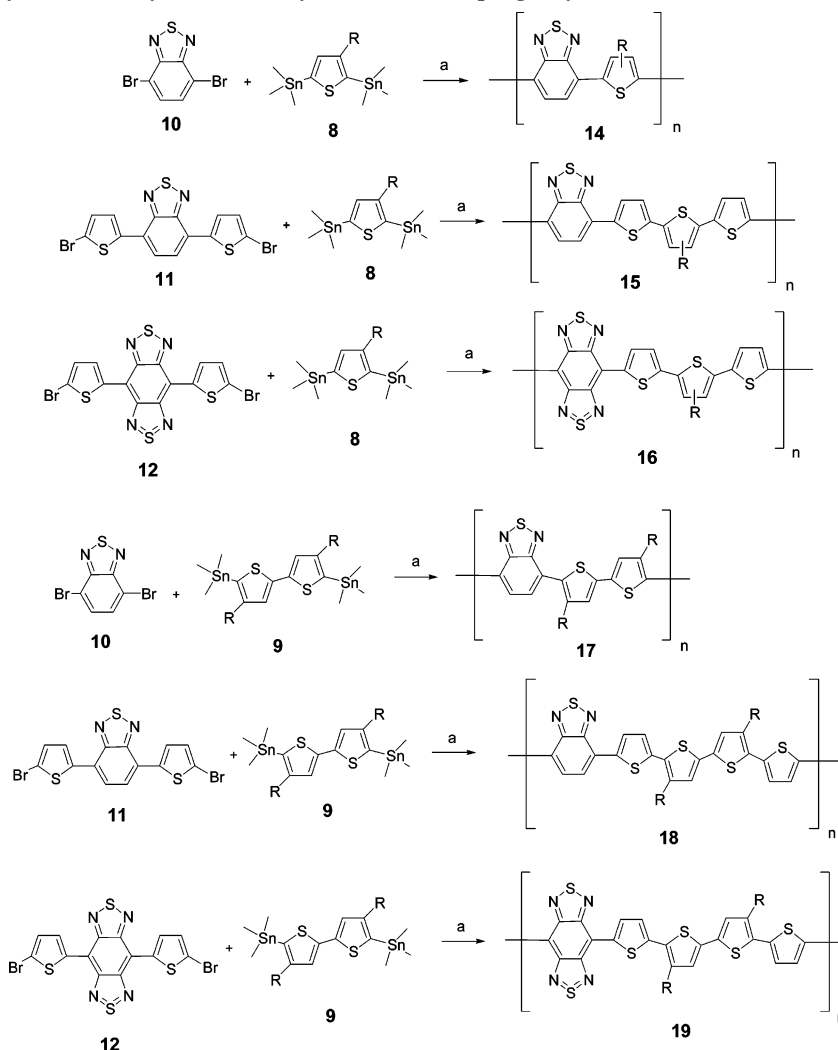
Scheme 7. Dibromo Derivates of Benzothiadiazole, **10** and **11**<sup>13,14</sup>



4,7-Bis(5-bromothiophen-2-yl)-2λ<sup>4</sup>δ<sup>2</sup>-benzo[1,2-*c*:4,5-*c'*]bis[1,2,5]thiadiazole (**12**) was synthesized from 4,8-dithien-2-yl-2λ<sup>4</sup>δ<sup>2</sup>-benzo[1,2-*c*:4,5-*c'*]bis[1,2,5]thiadiazole (Scheme 8).<sup>15,16</sup> The synthesis with NBS was carried out in both DMF and a 1:1 mixture of chloroform and acetic acid. Because of insolubility of the starting material in DMF, the tetra-brominated

Scheme 8. Synthesis of **12**<sup>a</sup><sup>a</sup> (a): NBS, CHCl<sub>3</sub>/AcOH.Scheme 9. Synthesis of Monomer for Ferric Chloride Polymerization<sup>a</sup><sup>a</sup> a: Pd(PPh<sub>3</sub>)<sub>2</sub>Cl<sub>2</sub>, THF, reflux.

benzobis(thiadiazole), 4,7-bis(dibromothiophen-2-yl)benzo[2,1,3]bis(thiadiazole), was obtained as a byproduct. Refluxing the starting material for 2 h in chloroform before adding acetic acid and NBS gave the pure product **12**. Because of the insolubility of **12**, the <sup>1</sup>H NMR spectra could only be obtained in high boiling NMR solvent mixtures at elevated temperature. A mixture of 1,2-dichlorobenzene-*d*<sub>4</sub>/*N,N*-dimethylformamide-*d*<sub>7</sub> (1:1) at 400 K was found to be suitable.

Scheme 10. Synthesis of Polymers **14–19** by Stille Cross-Coupling Polymerization, R = 3,7,11-Trimethyldodecyl<sup>a</sup><sup>a</sup> a: Pd(PPh<sub>3</sub>)<sub>2</sub>Cl<sub>2</sub>, DMF/THF, 150 °C.

**Stille Coupling.** Compound **11**<sup>13</sup> was reacted with **4** in a Stille cross-coupling to give 4,7-bis(2-ethylhexyl-2,2'-thiophen-5-yl)-benzo[2,1,3]thiadiazoles (**13**) (Scheme 9).

**Synthesis of Polymer Products.** *Stille Cross-Coupling Polymerization.* The polymers **14–19** were synthesized by Stille cross-coupling polymerization between dibromo derivatives of benzothiadiazole or benzobis(thiadiazole) and distannyl derivatives of 3-(3,7,11-trimethyldodecyl)thiophene or 4,4'-bis(3,7,11-trimethyldodecyl)dithiophene compounds (Scheme 10).

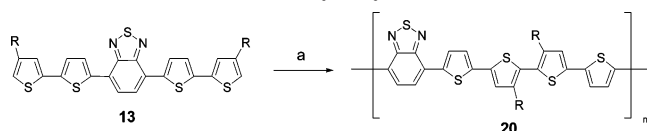
The monomers were heated in DMF, and the palladium catalyst was added. After a few hours a prepolymer had precipitated, and THF was added to dissolve the prepolymer<sup>17</sup> and continue the polymerization. After 2–3 days the polymers were precipitated with methanol and water. Determination of the amount of palladium in polymers synthesized from a palladium catalyzed polymerization was described by Nielsen et al.<sup>18</sup> A method for the removal of palladium from the polymer product was also reported.<sup>18</sup> Analysis of polymer **14–19** showed a palladium content of less than 100 ppm in the polymer. The polymers **14–19** were further purified by Soxhlet extraction with successively MeOH, hexane, and chloroform. The chloroform fraction was recovered and concentrated before further purification by preparative SEC. The SEC data of the purified polymers are summarized in Table 1.

Table 1. SEC Data of Purified Polymers 14–19<sup>a</sup>

polymer	$M_w$	$M_p$	$M_w/M_n$
14	5800	4800	1.4
15	2300	2100	1.3
16	7100	8600	1.9
17	9400	9500	1.8
18	14000	12000	1.9
19	12000	11000	2.1

<sup>a</sup> The polymers were analyzed on a gel column system comprising of a succession of columns with 500, 10 000, and 1 000 000 Å pore size with a detector wavelength of 500 nm. The SEC traces are given in the Supporting Information.

**Oxidative Ferric Chloride Polymerization.** The polymerization of **13** was carried out using ferric(III) chloride in chloroform to give the polymer **20** (Scheme 11).

Scheme 11. Oxidative Ferric Chloride Polymerization To Give Head-to-Head Copolymers of Dithiophene and Benzothiadiazole, R = 2-Ethylhexyl (20)<sup>a</sup>

<sup>a</sup> a: FeCl<sub>3</sub>, CHCl<sub>3</sub>.

Table 2. SEC Data of the Purified Polymer 20<sup>a</sup>

polymer	$M_w$	$M_p$	$M_w/M_n$
20	86 000	60 000	2.0

<sup>a</sup> The polymer was analyzed on a gel column system comprising a succession of columns with 500, 10 000, and 1 000 000 Å pore diameter with a detector wavelength of 500 nm. The SEC trace of the polymer is given in the Supporting Information.

The monomer was dissolved in chloroform and added to the ferric(III) chloride in chloroform. The solution was refluxed for 25 h; the resulting polymer was purified with aqueous sulfuric acid and aqueous sodium sulfite. It was not possible to establish whether complete removal of iron species was achieved. Polymer **20** was further purified by preparative SEC, and the SEC data are summarized in Table 2.

**Film-Forming Ability and Solubility.** The film-forming ability of polymers **14–20** was tested in different solvents by spin-coating the polymer solutions onto glass slides with subsequent measurement of the absorbance. Absorbencies of at least 0.3 at  $\lambda_{\max}$  were required to ensure a sufficiently thick film for photovoltaic studies or other thin-film studies. The analysis showed that the film-forming ability of polymers **14–20** is good in solvents like chloroform and THF.

Synthesis of polymers **14–16** with 2-ethylhexyl side chains, polymers **17–19** with hexyl side chains in a head-to-tail coupling, and polymer **20** with hexyl or dodecyl side chains is described in detail in the Supporting Information. Analyses of these polymers showed poor film-forming ability in CHCl<sub>3</sub>, THF, chlorobenzene, dichlorobenzene, xylene, and toluene. Hence, these polymers were not good enough to produce films with a sufficient quality for photovoltaic studies or other thin-film studies. Further, because of the poor solubility of these polymers, SEC data did not give a correct picture of the polymer molecular weight distribution, and the data are not reported.

From these results, it can be concluded that the long and branched alkyl chain, 3,7,11-trimethyldodecyl, resulted in soluble polymer products compared to polymer products bearing hexyl, 2-ethylhexyl (with the exception of polymer **20**), or dodecylalkyl side chains.

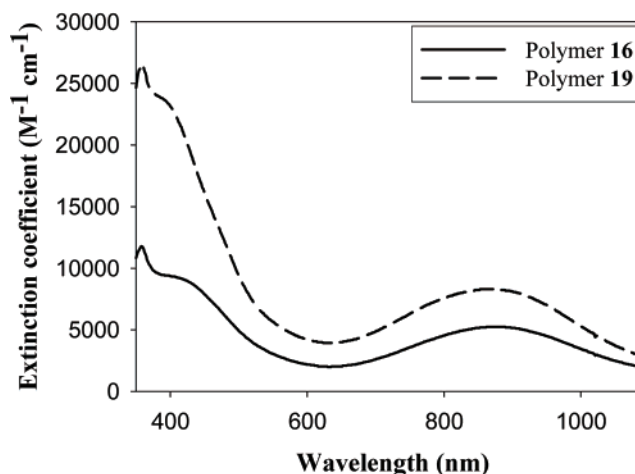
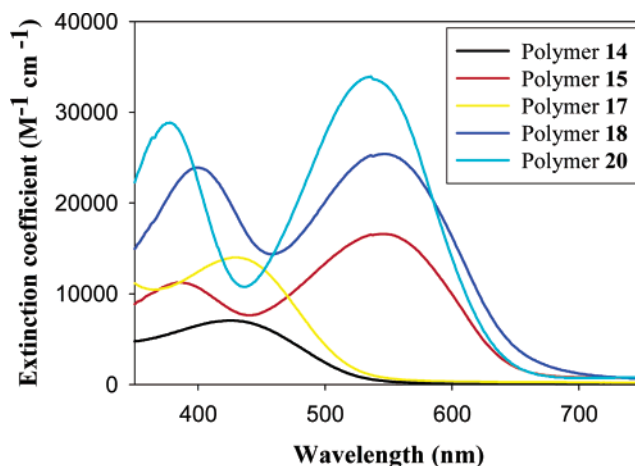


**Figure 1.** UV-vis spectra of polymers **14–20** in chloroform (360–1100 nm). We did not observe any significant red or blue shift when comparing spectra measured in solution and on film.

Table 3. Extinction Coefficients at  $\lambda_{\max}$  for the Polymers 14–20

	14	15	16	17	18	19	20
$\lambda_{\max}$ (nm)	477	435 602	770	479	450 597	902	428 586
$\epsilon$ (M <sup>-1</sup> cm <sup>-1</sup> )	7056	11228 165909	7609	14000	23994 25420	8081	28871 33957

**UV-vis.** The UV-vis spectra from  $\lambda = 360$  nm to  $\lambda = 1100$  nm of polymers **14–20** are shown in Figure 1.

The extinction coefficients at  $\lambda_{\max}$  for polymers **14–20** are listed in Table 3. From Table 3 and Figure 1, it can be seen that polymer **18** has a larger extinction coefficient at  $\lambda_{\max}$  than polymers **14**, **15**, **16**, **17**, and **19**. It can also be seen that  $\lambda_{\max}$  is red-shifted for the polymers synthesized from dithiophene (polymers **17–19**) compared to polymers synthesized from thiophene (polymers **14–16**). Further, it can be seen that polymer **20** has a larger extinction coefficient at  $\lambda_{\max}$  than polymer **18** and that  $\lambda_{\max}$  for polymer **20** is red-shifted compared to polymer **18**. This could be due to the different dithiophene coupling in the polymers **18** and **20**, i.e., tail-to-tail and head-to-head, respectively.

Further, it can be seen that polymers **16** and **19** show absorption above 1100 nm. In Figure 2 the UV-vis and NIR spectra of polymers **16** and **19** are shown from 800 to 2500 nm. From these data, it can be seen that polymers **16** and **19** absorb significantly up to around 1800 nm.

Band gaps ( $E_g$ ) were estimated from UV-vis spectra by fitting a tangent to the UV curve with subsequent conversion



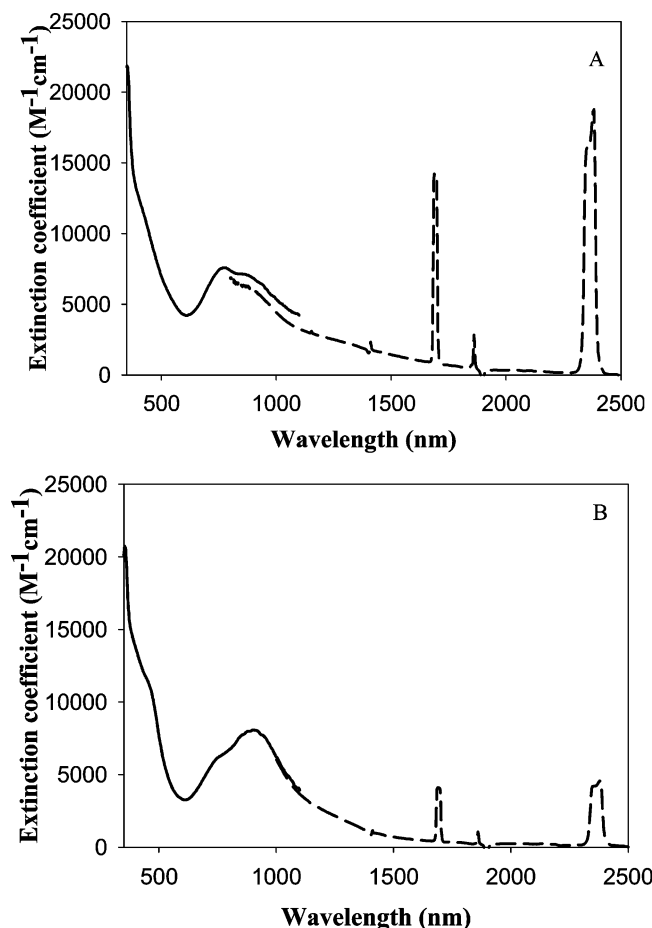


**Figure 2.** UV-vis (black) and NIR (dashed) for polymers **16** (A) and **19** (B). The peaks at 1400, 1600, 1900, and 2400 nm are due to the instrument.

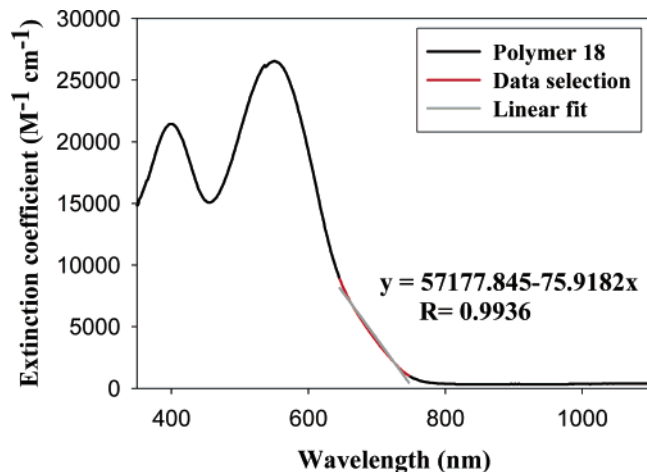


**Figure 3.** Band-gap estimation of polymer **18**.

of the intersection with the wavelength axis ( $x_0$ ) from nm to eV (an example is given in Figure 3 with polymer **18**). Because of the tailing of the absorption toward longer wavelengths (especially for polymers **16** and **19**), the exact position of the optical band gap was found to be difficult to establish. We have used a conservative measure for the optical band gap, and actual values may be lower.

The band gaps are listed in Table 4. The polymers described in the literature show band gaps of 2.0 eV for polythiophene,<sup>19</sup> 1.6 eV for copolymers of thiophene, pyrrole, and benzothiadiazole,<sup>2,4</sup> and 1.2 eV for polyisothianaphthene.<sup>6</sup> Comparing these polymers with polymers **14–20** shows that polymers **14**

and **17** have band gaps in the same region as polythiophene,<sup>19</sup> polymer **15** has a band gap in the region between polythiophene and copolymers of thiophene, pyrrole, and benzothiadiazole, and polymers **18** and **20** have band gaps in the same region as copolymers of thiophene, pyrrole, and benzothiadiazole.<sup>2,4</sup> Further, it can be seen that polymers **16** and **19** have lower band gaps than polyisothianaphthene.<sup>6</sup>

**Ultraviolet Photoelectron Spectroscopy (UPS).** The electronic structure of the materials was established by a combination of the band-gap data presented above and UPS. UPS employs the irradiation of a thin film of the sample on a metal substrate with high-energy UV photons. In the experiments performed here the incident photon energy was 50 eV. The high-energy photons result in photoelectrons that are collected and their energy measured. This gives a photoelectron spectrum that provides a map of the filled energy levels in the material and the ionization potential. One advantage of using a synchrotron source is that ESCA/XPS can be recorded for the surface region used for UPS studies. This allows for the chemical analysis, and thus one can make sure that no impurities are present and confirm the presence of the elements that are expected (in this case carbon, sulfur, and nitrogen). The method for the analysis of the UPS data has been reported earlier.<sup>20,21</sup>

The UPS spectrum and the band-gap structure of polymers **17–19** are shown in Figure 4 along with a sketch of the band structure. The UPS spectrum and band-gap structure of polymers **14–16** and **20** are given in the Supporting Information. The results obtained by the UPS measurements on polymers **14–20** are shown in Table 4.

The values were obtained from the following equations:<sup>20,21</sup>

$$\Phi_{\text{Au}} = h\nu - \text{BE}_{\text{max}} \quad (1)$$

$$E_{\text{F}}^{\text{VB}} = \text{BE}_{\text{min}} \quad (2)$$

$$E_{\text{F}}^{\text{VAC}} = h\nu - \text{BE}_{\text{max}} \quad (3)$$

$$\text{IP} = E_{\text{F}}^{\text{VB}} + E_{\text{F}}^{\text{VAC}} \quad (4)$$

$$\Delta = E_{\text{F}}^{\text{VAC}} - \Phi_{\text{Au}} \quad (5)$$

where  $\text{BE}_{\text{max}}$  and  $\text{BE}_{\text{min}}$  are the cutoff at high binding energy and the onset at low binding energy, respectively.  $\text{BE}_{\text{min}}$  represents the injection barrier for holes from gold into the valence band of the polymer material ( $E_{\text{F}}^{\text{VB}}$ ). The work function of the substrate ( $\Phi_{\text{Au}}$ ) is obtained from eq 1, where  $\text{BE}_{\text{max}}$  is obtained by measurements on a clean sample, where the Fermi level of gold is established.  $E_{\text{F}}^{\text{VAC}}$  is the distance from the Fermi level to the vacuum level and is obtained from eq 3. IP, the ionization potential, is a material constant, and  $\Delta$  is the vacuum level shift, i.e., the effect of the dipole layer at the interface of vacuum and the polymer layer.<sup>20,21</sup>

ESCA measurements showed no gold in the samples, indicating that the films were thick enough for the UPS measurements. Furthermore, a variation of the illuminated spot size and counting times gave the same UPS spectrum, thus eliminating the possibility of too thick films giving rise to surface charging.

In the UPS experiment the Fermi level of the polymer material aligns with the Fermi level of the metal substrate. For pure semiconductors the Fermi level of the material should be in the middle of the (forbidden) optical band gap and the distance from the Fermi level to the topmost filled electronic energy level should thus be half the value for the optical band gap. In reality, this is known to vary due to impurities in the samples, and the

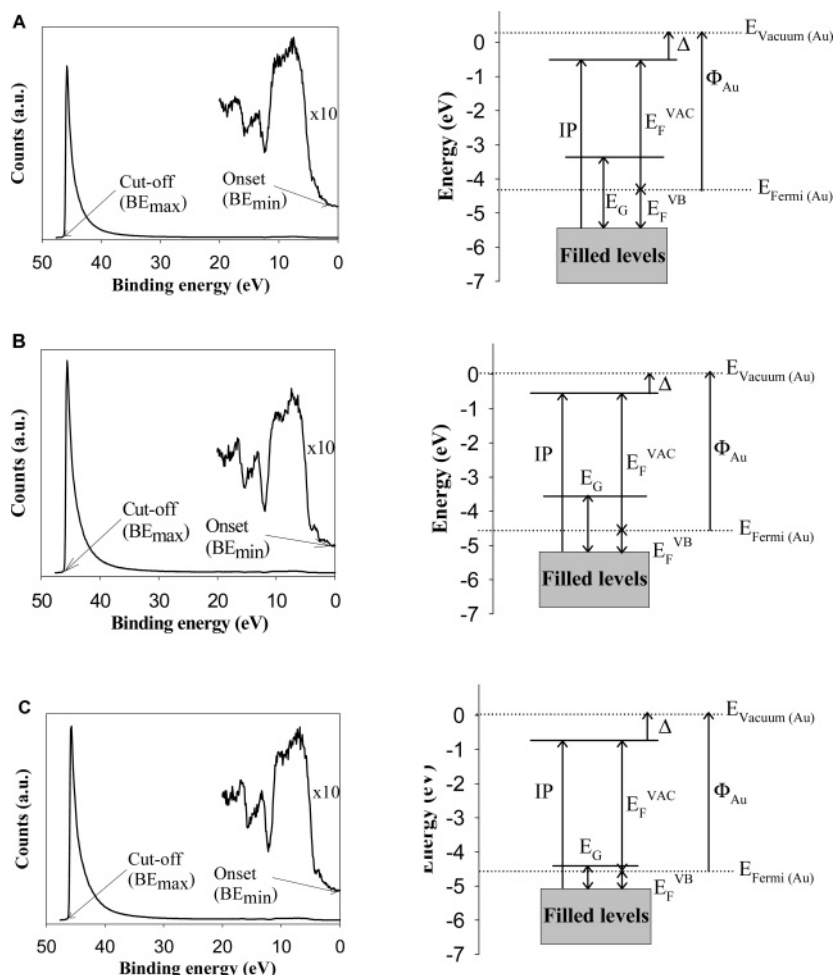


**Figure 4.** UPS spectra (left) and the resulting band structure (right) for polymers **17** (A), **18** (B), and **19** (C).

**Table 4. Band-Gaps from UV–Vis Spectra and UPS Data from the Photoelectron Spectra for Polymers 14–20<sup>a</sup>**

polymer	$E_F^{VB}$ (eV)	$E_F^{VAC}$ (eV)	$I_p$ (eV)	$\Delta$ (eV)	$E_G$ (eV)
<b>14</b>	1.44	3.96	5.40	−0.64	2.10
<b>15</b>	0.80	4.04	5.84	−0.56	1.82
<b>16</b>	0.52	3.92	4.44	−0.68	0.65
<b>17</b>	1.11	3.81	4.92	−0.79	2.10
<b>18</b>	0.63	4.04	4.67	−0.56	1.65
<b>19</b>	0.48	3.86	4.34	−0.74	0.67
<b>20</b>	1.19	3.88	5.07	−0.72	1.77

<sup>a</sup>  $E_G$  values are estimated from UV–vis spectra.

buried interface between the material and the metal substrate may shift the position of the Fermi level away from the midpoint. The ionization potential is also a direct observable from the experiment and is dependent upon the molecular orientation at the surface between the materials and vacuum. The orientation of the molecular dipoles may facilitate the escape of a photoelectron or hinder the escape. This effect is observed through the vacuum level shift,  $\Delta$ , that most often acquires a slightly negative value.<sup>22</sup> The distance from the Fermi level to the topmost filled electronic energy levels,  $E_F^{VB}$ , represents the barrier to the injection of holes from the metal substrate into the valence band of the conjugated polymer material.

The general observation is that the Fermi level of the material aligns quite well with the middle of the optical band gap (Figure 4). In the case of the copolymers of thiophene and benzobis(thiadiazole), **16** and **19**, the value for  $E_F^{VB}$  is significantly larger than half the value of  $E_G$ . This can be indicative of a slight amount of n-doping or an underestimation of the value for the band gap. UV–vis data for both these materials, however, show

low band gap values. The low values observed for  $E_F^{VB}$  thus support our proposition of a very low band gap for these materials. Dedoping experiments with hydrazine and ammonia were attempted to establish whether the very low band gap polymers, **16** and **19**, or the polymer that exhibited a tail in the absorption spectrum, **18**, were doped. This however did not change the absorption spectrum, and we conclude that the doping of the materials if present cannot be removed simply by a treatment with a chemical reducing agent (see Supporting Information). Further, we observe emission from polymer **18** and therefore assume that the impurity level is low since doping is known to efficiently quench emission (see Supporting Information). On the basis of this, we may have underestimated the band gap for the polymers **16** and **19**, and assuming that the optical band gap should be twice the value for  $E_F^{VB}$ , the values for the band gaps would be 0.96 and 1.04 eV, respectively. We consider these values as upper bounds on the values for the band gap. Since the UPS experiment does not probe the empty electronic energy levels, however, the values for  $E_G$  are still most reliably obtained from the UV–vis experiment.

If the band gap  $E_G$  and the  $E_F^{VB}$  are plotted as a function of the number of thiophene units in the monomer for the polymers based on benzothiadiazole (Figure 5), it can be seen that the band gap  $E_G$  decreases when the number of thiophene units is increased. This tendency also applies for  $E_F^{VB}$ . Hence, the injection barrier for holes from the metal substrate into the polymer material is lower when the number of thiophene units is larger,  $n = 4$ , and at the same time the band gap is lowered.

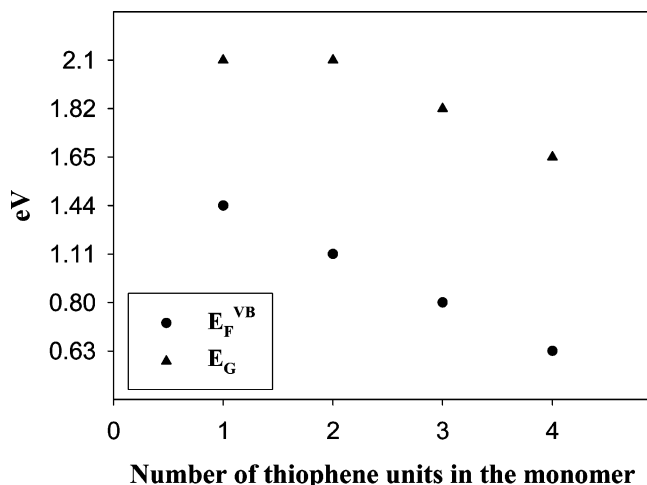


**Figure 5.**  $E_F^{VB}$  and  $E_G$  plotted as a function of the number of thiophene units in the monomer.

## Conclusion

We have presented the synthesis of a series conjugated copolymers of thiophene and benzothiadiazole and benzobis(thiadiazole). Molecular weight, solubility, and film-forming ability were highly dependent on which side chain was used. Hexyl, 2-ethylhexyl, and dodecyl side chains gave polymer products with low molecular weight and poor solubility. We found that 3,7,11-trimethyldodecyl side chains gave polymer products with higher molecular weight, good solubility, and film-forming ability. Polymer products were characterized by SEC, UV-vis, and NMR. Band gaps were estimated by UV-vis to 2.1–1.7 eV for polymer based on benzothiadiazole and ~0.7 eV for polymers based on benzobis(thiadiazole). The electronic structures of polymers **14**–**20** were determined by a combination of UV-vis and UPS. This showed that both  $E_G$  and  $E_F^{VB}$  decrease with the increasing number of thiophenes in the monomer unit.

## Experimental Section

**General.** All commercially available reagents were purchased from Aldrich. 1-Bromo-3,7,11-trimethyldodecane,<sup>10</sup> 4,7-dibromo-2,1,3-benzothiadiazole (**10**),<sup>14</sup> 4,7-bis(5-bromothiophen-2-yl)-[2,1,3]-benzothiadiazole (**11**),<sup>13</sup> and 4,8-dithien-2-yl-2,4,6-benzo[1,2-c:4,5-c']bis[1,2,5]benzothiadiazole<sup>15,16</sup> were all synthesized according to the literature.

In <sup>13</sup>C NMR for compound **8** two signals are missing. This is ascribed to accidental isocrony.

Compounds **1**, **6**, **8**, and **9** contained 2,6,10,15,19,23-hexamethyltetraacosane as an impurity, and compounds **4** and **20** contained 5,8-diethyldodecane as an impurity. These alkane byproducts stem from the Würtz coupling of the alkyl halides during the Grignard reaction and are seen in the NMR spectra of the respective compounds. The products were attempted purified by chromatography and Kugelrohr distillation. It was in our hands impossible to remove these byproducts due to codistillation and very similar physical properties. Since these alkane products are neutral in terms of future chemical reactions, we chose to use these materials directly and could successfully remove the byproducts in subsequent steps.

**Photophysical.** The UV-vis spectra were recorded on an Shimadzu UV-1700 PharmaSpec. The NIR spectra were recorded on a Fourier transform infrared spectrometer (FTIR) Bomem/ABB model MB155. UV-vis and NIR spectra were obtained from chloroform solution. We did not observe any significant red or blue shift when comparing spectra measured on solution and film.

**Size exclusion chromatography (SEC)** was performed in chloroform using either of two preparative Knauer systems employing a precolumn and two gel columns in succession with respec-

tively pore diameters of 500, 10 000, and 1 000 000 Å. All gel columns had dimensions of 25 mm diameter × 600 mm. Polystyrene standards were used for molecular weight determination.

**Ultraviolet Photoelectron Spectroscopy (UPS).** Gold was evaporated on the aluminum substrates in a vacuum chamber at a pressure  $<5 \times 10^{-6}$  mbar. Hereafter, the 2.7 μm microfiltered polymer solutions were spin-coated on the substrate from chloroform or THF. The UPS measurements were carried out with 50 eV photons at the ASTRID synchrotron at University of Aarhus, Denmark. The setup of the experiment was described previously.<sup>23–25</sup>

**General Procedure for Addition of Alkyl Chain to Thiophene (Grignard Reaction).**<sup>11</sup> Magnesium turnings (0.31 mol) were crunched under argon for 30 min. Ether (250 mL) and iodine (to color change) were added. A few drops of bromoalkane were added, and the mixture left until the reaction started (heating with a heat gun and addition of a few drops of 1,2-dibromoethane helped to start the reaction). Once started (color change from orange to gray), bromoalkane (0.31 mol, 10% excess) was added dropwise, keeping the reaction at gentle reflux. After end addition the mixture was left stirring for 30 min. At this point the catalyst, Nidppp (225 mg) was added in one portion. After the foaming had subsided 3-bromothiophene (0.3 mol) was added dropwise, keeping the reaction mixture at gentle reflux. After each 1/4 of addition, further Nidppp (135 mg) was added. At the end of the addition, further Nidppp (135 mg) was added, and the mixture was left stirring overnight. The following day the mixture was hydrolyzed by careful addition of water (110 mL) for 1 h followed by 37% aqueous HCl (45 mL) for 30 min. The light brown organic phase was separated, dried (MgSO<sub>4</sub>), evaporated, distilled, and purified by flash chromatography (cyclohexane) to give the product.

**3-(3,7,11-Trimethyldodecyl)thiophene (1):** yield 61%, colorless oil, bp 120–123 °C at 5 mbar. <sup>1</sup>H NMR (250 MHz, CDCl<sub>3</sub>): δ = 7.25–7.22 (m, 1H), 6.95–6.92 (m, 2H), 2.68–2.59 (m, 2H), 1.70–1.01 (m, 17H), 0.98–0.79 (m, 12H). <sup>13</sup>C NMR (75 MHz, CDCl<sub>3</sub>): δ = 143.40, 128.24, 125.01, 119.61, 39.42, 37.91, 37.83, 37.46, 37.42, 37.34, 37.30, 37.26, 32.83, 32.52, 28.01, 27.89, 26.97, 24.84, 24.42, 22.73, 22.64, 19.78, 19.71, 19.64, 19.58.

**3-(2-Ethylhexyl)thiophene (2):** yield 95%, colorless oil, bp 150–152 °C at 10 mbar. <sup>1</sup>H NMR (250 MHz, CDCl<sub>3</sub>): δ = 7.22 (dd, 1H, *J* = 4.75, 3 Hz), 6.92–6.89 (m, 2H), 2.56 (d, 2H, *J* = 6.75 Hz), 1.60–1.50 (m, 1H), 1.34–1.18 (m, 10H), 0.92–0.80 (m, 7H) 3H too many. <sup>13</sup>C NMR (75 MHz, CDCl<sub>3</sub>): δ = 141.90, 128.77, 124.73, 120.59, 40.41, 34.30, 32.53, 28.90, 25.66, 22.99, 14.06, 10.81. MS (HRMS): *m/z* calcd for [C<sub>12</sub>H<sub>21</sub>S]<sup>+</sup> 197.1364; found 197.1238.

**General Procedure for Trialkylstannylation of Alkylthiophene with *n*BuLi and TMEDA.** Alkylthiophene (7 mmol) and TMEDA (10.5 mmol, 1.5 equiv) in hexane (50 mL) was cooled to –78 °C. *n*BuLi (10.5 mmol, 1.5 equiv) was added dropwise over 30 min. The cooling bath was removed, and the reaction was stirred at room temperature for 2 h. The reaction mixture was cooled back down to –78 °C, and trimethylstannyl chloride (17 mmol, 2.5 equiv) was added. After 1 h at room temperature, the mixture was washed with water, dried, evaporated, and purified by Kugelrohr distillation.

**2-(Trimethylstannyl)-4-(3,7,11-trimethyldodecyl)thiophene (3):** yield 54%, colorless oil, bp 175 °C at  $8 \times 10^{-3}$  mbar. <sup>1</sup>H NMR (250 MHz, CDCl<sub>3</sub>): δ = 7.20 (s, 1H), 7.01 (s, 1H), 2.77–2.55 (m, 2H), 1.72–1.01 (m, 19H), 0.93–0.84 (m, 13H), 0.47–0.24 (m, 9H). <sup>13</sup>C NMR (75 MHz, CDCl<sub>3</sub>): δ = 144.75, 137.24, 136.58, 125.49, 39.38, 38.06, 37.97, 37.43, 37.38, 37.30, 37.26, 37.23, 32.78, 32.63, 27.67, 27.52, 24.78, 24.39, 22.69, 22.60, 19.74, 19.68, 19.64, 19.58, –8.35.

**General Procedure for Trialkylstannylation of Alkylthiophene with LDA.**<sup>12,26</sup> LDA in THF/ethylbenzene/heptane (2 M, 0.2 mol) was added dropwise to a solution of alkylthiophene (0.2 mol) in dry THF (300 mL) cooled to –78 °C under argon. After the end of the addition the mixture was allowed to reach 0 °C for 3 h. The mixture was then cooled back down to –78 °C, and tributylstannyl chloride (0.2 mol) was added in one portion. The brown color disappeared, and the temperature rose to –40 °C. The mixture was allowed to reach room temperature. Hexane was added



to the reaction mixture, and it was washed with water, dried (MgSO<sub>4</sub>), filtered, evaporated, and purified by Kugelrohr distillation.

**4-(2-Ethylhexyl)-2-tributylstannylthiophene (4):** yield 42%, yellow oil, bp 140 °C at  $3 \times 10^{-3}$  mbar. <sup>1</sup>H NMR (250 MHz, CDCl<sub>3</sub>):  $\delta$  = 7.16 (s, 1H), 6.93 (s, 1H), 2.60 (d, 2H,  $J$  = 3.5 Hz), 1.73–1.46 (m, 10H), 1.43–1.89 (m, 20H), 1.57–1.00 (m, 8H), 0.98–0.85 (m, 20H). <sup>13</sup>C NMR (75 MHz, CDCl<sub>3</sub>):  $\delta$  = 142.98, 137.43, 135.83, 126.32, 40.56, 33.95, 32.60, 28.95, 28.19, 27.84, 27.20, 25.79, 23.03, 16.41, 14.07, 13.60, 10.89, 10.77.

**4,4'-Bis(3,7,11-trimethyldodecyl)-2,2'-dithiophene (6):** 3-(3,7,11-Trimethyldodecyl)thiophene (4.0 g, 13.6 mmol) in THF (100 mL) was cooled to –78 °C. *n*BuLi (21.26 mL, 34.0 mmol, 2.5 equiv) was added dropwise. The temperature rose to –40 °C. After stirring for 10 min, I<sub>2</sub> in THF was added until the color changed to weak yellow. The reaction was allowed to reach room temperature. Pd(PPh<sub>3</sub>)<sub>2</sub>Cl<sub>2</sub> (600 mg, 0.9 mmol) was added, and the mixture was heated to reflux. 2-(Trimethylstannyl)-4-(3,7,11-trimethyldodecyl)-thiophene (5.596 g, 12.2 mmol) was added dropwise for 30 min. The reaction was left stirring overnight under reflux. The reaction mixture was evaporated, filtered through silica (hexane), and purified by Kugelrohr distillation. Yield 55% (4.39 g), green oil, bp 275 °C at  $3 \times 10^{-3}$  mbar. <sup>1</sup>H NMR (250 MHz, CDCl<sub>3</sub>):  $\delta$  = 6.94 (d, 2H,  $J$  = 1 Hz), 6.77 (d, 2H,  $J$  = 1 Hz), 2.68–2.44 (m, 4H), 1.70–1.01 (m, 40H), 0.96–0.76 (m, 27H). <sup>13</sup>C NMR (75 MHz, CDCl<sub>3</sub>):  $\delta$  = 144.23, 137.42, 124.80, 118.56, 39.39, 37.72, 37.63, 37.43, 37.39, 37.30, 37.25, 37.21, 32.78, 32.47, 28.10, 27.97, 24.79, 24.38, 22.70, 22.61, 19.75, 19.69, 19.61, 19.56. MS (HRMS):  $m/z$  calcd for [C<sub>38</sub>H<sub>67</sub>S<sub>2</sub>]<sup>+</sup> 587.4679; found 587.4705.

**3-(3,7,11-Trimethyldodecyl)-2,5-bis(trimethylstannyl)thiophene (8):** 3-(3,7,11-Trimethyldodecyl)thiophene (1 g, 3.4 mmol) in hexane (25 mL) was cooled to –78 °C. *t*BuLi (10.0 mL, 17 mmol) was added dropwise over 30 min (yellow solution). The cooling bath was removed, and the reaction was stirred at room temperature for 3½ days (yellow suspension). The mixture was cooled back down to –78 °C, and trimethylstannyl chloride in hexane (23.8 mL, 23.8 mmol) was added (yellow to white suspension). After 1 h at room temperature, the mixture was washed with water, dried, evaporated, and purified by Kugelrohr distillation. Yield: 57% (1.2 g), yellow oil, bp 200 °C at  $4 \times 10^{-3}$  mbar. <sup>1</sup>H NMR (250 MHz, CDCl<sub>3</sub>):  $\delta$  = 7.19 (s, 1H), 2.78–2.57 (m, 2H), 1.69–1.02 (m, 24H), 0.96–0.84 (m, 15H), 0.49–0.24 (m, 18H). <sup>13</sup>C NMR (75 MHz, CDCl<sub>3</sub>):  $\delta$  = 152.13, 143.13, 137.45, 39.83, 39.74, 39.39, 37.46, 37.41, 37.32, 33.18, 32.82, 29.81, 27.98, 24.81, 24.47, 22.71, 22.62, 19.76, 19.70, –7.96, –8.21. MS (HRMS):  $m/z$  calcd for [C<sub>25</sub>H<sub>50</sub>SSn<sub>2</sub>Na]<sup>+</sup> 643.1597; found 643.2317.

**4,4'-Bis(3,7,11-trimethyldodecyl)-5,5'-bis(trimethylstannyl)-2,2'-dithiophenyl (9):** 4,4'-Bis(3,7,11-trimethyldodecyl)-2,2'-dithiophene (2 g, 3.4 mmol) and TMEDA (1.53 mL, 10.2 mmol, 3 equiv) in hexane (50 mL) was cooled to –78 °C. *n*BuLi (6.38 mL, 10.2 mmol, 3 equiv) was added dropwise over 30 min (orange solution). The cooling bath was removed, and the reaction was stirred at room temperature for 1 h (light orange suspension). The mixture was cooled back down to –78 °C, and trimethylstannyl chloride (17 mL, 17.0 mmol, 5 equiv) was added (yellow solution). After 1 h at room temperature (yellow suspension), the mixture was washed with water, dried, evaporated, and purified by Kugelrohr distillation. Yield: 75% (2.34 g), yellow oil, bp 250 °C at  $3 \times 10^{-3}$  mbar. <sup>1</sup>H NMR (250 MHz, CDCl<sub>3</sub>):  $\delta$  = 7.11 (s, 2H), 2.69–2.47 (m, 4H), 1.68–1.03 (m, 42H), 0.97–0.83 (m, 28H), 0.50–0.27 (18H, m). <sup>13</sup>C NMR (75 MHz, CDCl<sub>3</sub>):  $\delta$  = 151.77, 142.76, 130.75, 126.01, 39.50, 39.38, 37.44, 37.40, 37.35, 37.31, 33.01, 32.81, 30.51, 27.97, 24.80, 24.45, 22.71, 22.62, 19.76, 19.73, 19.70, 19.68, –7.89.

**4,7-Bis(5-bromothiophen-2-yl)-2,2'-bis-benzo[1,2-*c*;4,5-*c'*]bis-[1,2,5]thiadiazole (12):** NBS (903.1 mg, 5.1 mmol, 2.5 equiv) in CHCl<sub>3</sub>/AcOH (5 mL) was added dropwise to a solution of 4,8-dithien-2-yl-2,2'-bis-benzo[1,2-*c*;4,5-*c'*]bis[1,2,5]benzothiadiazole (728.3 mg, 2 mmol) in CHCl<sub>3</sub>/AcOH (1 L) in darkness. After 2½ h the mixture was filtered and recrystallized from DMF. Yield: 83% (870.3 mg), green solid. <sup>1</sup>H NMR (250 MHz, 1,2-dichlorobenzene-*d*<sub>4</sub>/*N,N*-dimethylformamide-*d*<sub>7</sub> 1:1, 400 K):  $\delta$  = 8.92 (d, 1H,  $J$  = 4

Hz), 7.48 (d, 1H,  $J$  = 4 Hz). UV–vis (CHCl<sub>3</sub>)  $\lambda_{\text{max}}$  735 nm (log  $\epsilon$  4.40). Anal. Calcd for C<sub>14</sub>H<sub>4</sub>Br<sub>2</sub>N<sub>4</sub>S<sub>4</sub>: C, 32.57; H, 0.78; N, 10.85. Found: C, 33.44; H, 0.64; N, 10.84.

**General Procedure for Stille Coupling:**<sup>12,15,16</sup> To a solution of the dibromo compound (1.0 mmol) and 2-(tributylstannyl)thiophene (2.5 mmol) in THF (3.5 mL), Pd(PPh<sub>3</sub>)<sub>2</sub>Cl<sub>2</sub> ( $6.25 \times 10^{-2}$  mmol) was added. The mixture was refluxed until the reaction terminated, after which it was washed, cooled, evaporated, and purified by flash chromatography and recrystallized.

**4,7-Bis(4'-(2-ethylhexyl)-2,2'-dithiophenyl-5-yl)benzo[1,2,5]-thiadiazole (13):** yield 37%, dark red oil. <sup>1</sup>H NMR (250 MHz, CDCl<sub>3</sub>):  $\delta$  = 8.03 (d, 2H,  $J$  = 4 Hz), 7.86 (s, 2H), 7.25 (d, 2H,  $J$  = 4 Hz), 7.12 (d, 2H,  $J$  = 1 Hz), 6.84 (d, 2H,  $J$  = 1 Hz), 2.55 (d, 4H,  $J$  = 7 Hz), 1.69–1.58 (m, 2H), 1.37–1.31 (m, 16H), 0.91 (t, 12H,  $J$  = 7.25 Hz). <sup>13</sup>C NMR (75 MHz, CDCl<sub>3</sub>):  $\delta$  = 152.50, 143.06, 139.32, 137.75, 136.64, 128.18, 125.90, 125.56, 125.11, 124.19, 120.42, 40.30, 34.63, 32.53, 28.90, 25.66, 23.02, 14.09, 10.83. Anal. Calcd for C<sub>38</sub>H<sub>44</sub>N<sub>2</sub>S<sub>5</sub>: C, 66.23; H, 6.44; N, 4.07. Found: C, 66.13; H, 6.28; N, 3.86.

**General Procedure for Stille Cross-Coupling Polymerization.** Bis(stannyl)alkylthiophene (0.5 mmol) and dibromo compound (0.5 mmol) were mixed in DMF (150 mL, fresh bottle). The mixture was degassed with argon, and Pd(PPh<sub>3</sub>)<sub>2</sub>Cl<sub>2</sub> (30 mg) was added. The mixture was heated to 150 °C. After a prepolymer had precipitated, THF (75 mL) was added, and the reaction was stirred at 150 °C for 3–4 days. The suspension was evaporated, and the polymer was precipitated with MeOH/H<sub>2</sub>O (1–1.5 L). The suspension was filtered to give the polymer, which was purified by Soxhlet extraction with MeOH, hexane, and chloroform. The chloroform fraction was evaporated, and further purification was carried out by preparative SEC. The polymer was purified from Pd particles as described in the literature.<sup>18</sup>

**Poly{(benzo-2,1,3-thiadiazol-4,7-diyl)-(4-(3,7,11-trimethyldodecyl)thiophen-2-yl)} (14):** yield 54%. <sup>1</sup>H NMR (250 MHz, CDCl<sub>3</sub>):  $\delta$  = 8.24–7.33 (m, 1.5H), 7.18–6.81 (m, 0.5H), 3.10–2.34 (m, 2H), 1.91–1.12 (m, 17H), 1.12–1.063 (m, 12H). UV–vis: (CHCl<sub>3</sub>, nm) 477 (log  $\epsilon$  3.85). SEC (500 Å + 10 000 Å + 1 000 000 Å)  $M_w$  = 5824;  $M_p$  = 4803;  $M_w/M_n$  = 1.436. Contained <100 ppm Pd particles.

**Poly{(benzo-2,1,3-thiadiazol-4,7-diyl)-(4'-(3,7,11-trimethyldodecyl)-2,2';5',2''-tertthiophen-5,5'-diyl)} (15):** yield 60%. <sup>1</sup>H NMR (250 MHz, CDCl<sub>3</sub>):  $\delta$  = 8.22–7.67 (m, 3H), 7.51–7.30 (m, 1H), 7.24–6.82 (m, 3H), 3.09–2.67 (m, 2H), 1.85–1.00 (m, 34H, 17 too many H<sub>2</sub>O), 0.95–0.83 (m, 12H). UV–vis: (CHCl<sub>3</sub>, nm) 435, 602 (log  $\epsilon$  4.05, 5.22). SEC (500 Å + 10 000 Å + 100 000 Å)  $M_w$  = 2289;  $M_p$  = 2099;  $M_w/M_n$  = 1.280. Contained <100 ppm Pd particles.

**Poly{(benzo-2,1,3-bis-thiadiazol-4,7-diyl)-(4'-(3,7,11-trimethyldodecyl)-2,2';5',2''-tertthiophen-5,5'-diyl)} (16):** yield 83%. <sup>1</sup>H NMR (250 MHz, CDCl<sub>3</sub>):  $\delta$  = 9.12–8.58 (m, 0.5H), 8.13–7.61 (m, 0.5H), 7.42–7.31 (m, 1.5H), 7.16–6.62 (m, 2H), 2.88–2.17 (m, 2H), 1.88–0.98 (m, 17H), 0.98–0.60 (m, 12H). UV–vis: (CHCl<sub>3</sub>, nm) 770 (log  $\epsilon$  3.88). NIR: (CHCl<sub>3</sub>, nm) tail to 1800. SEC (500 Å + 10 000 Å + 1 000 000 Å)  $M_w$  = 7095;  $M_p$  = 8594;  $M_w/M_n$  = 1.860. Contained <100 ppm Pd particles.

**Poly{(benzo-2,1,3-thiadiazol-4,7-diyl)-(4,4'-di(3,7,11-trimethyldodecyl)-2,2'-dithiophen-5,5'-diyl)} (17):** yield 69%. <sup>1</sup>H NMR (250 MHz, CDCl<sub>3</sub>):  $\delta$  = 7.71 (s, 1H), 7.18–7.13 (m, 1H), 3.13–2.38 (m, 4H), 1.69–0.86 (m, 34H), 0.86–0.61 (24H). UV–vis: (CHCl<sub>3</sub>, nm) 479 (log  $\epsilon$  4.15). SEC (500 Å + 10 000 Å + 1 000 000 Å)  $M_w$  = 9368;  $M_p$  = 9461;  $M_w/M_n$  = 1.807. Contained <100 ppm Pd particles.

**Poly{(benzo-2,1,3-thiadiazol-4,7-diyl)-(3',4''-di(3,7,11-trimethyldodecyl)-2,2';5',2'';5'',2'''-quaterthiophen-5,5'-yl)} (18):** yield 93%. <sup>1</sup>H NMR (250 MHz, CDCl<sub>3</sub>):  $\delta$  = 8.22–8.01 (m, 1H), 7.93–7.75 (m, 1H), 7.12–6.78 (m, 2H), 2.96–2.48 (m, 4H), 1.80–0.84 (m, 63H). UV–vis: (CHCl<sub>3</sub>, nm) 450, 597 (log  $\epsilon$  4.38, 4.41). SEC (500 Å + 10 000 Å + 1 000 000 Å)  $M_w$  = 13 861;  $M_p$  = 12 250;  $M_w/M_n$  = 1.880. Contained <100 ppm Pd particles.

**Poly{(benzo-2,1,3-bis-thiadiazol-4,7-diyl)-(3',4''-di(3,7,11-trimethyldodecyl)-2,2';5',2'';5'',2'''-quaterthiophen-5,5'-yl)} (19):**



yield quant.  $^1\text{H}$  NMR (250 MHz,  $\text{CDCl}_3$ ):  $\delta$  = 9.08–8.90 (m, 1H), 7.80–7.59 (m, 1H), 7.41–7.30 (m, 1H), 7.21–6.78 (m, 1H), 2.79–2.55 (m, 4H), 1.90–1.09 (m, 60H, 26 too many), 1.09–0.61 (m, 34H, 10 too many). UV–vis: ( $\text{CHCl}_3$ , nm) 902 ( $\log \epsilon$  3.91). NIR: ( $\text{CHCl}_3$ , nm) tail to 1800. SEC (500 Å + 10 000 Å + 1 000 000 Å)  $M_w$  = 11 705;  $M_p$  = 10 819;  $M_w/M_n$  = 2.061. Contained <100 ppm Pd particles.

**General Procedure for Oxidative Ferric Chloride Polymerization.**<sup>17</sup> The monomer (0.5 mmol) in  $\text{CHCl}_3$  (10 mL) was added dropwise to a mixture of  $\text{FeCl}_3$  (1.26 mmol) in  $\text{CHCl}_3$  (150 mL). After 25 h of reflux the reaction was cooled, washed with aqueous  $\text{H}_2\text{SO}_4$  and aqueous  $\text{Na}_2\text{SO}_3$ , dried ( $\text{MgSO}_4$ ), filtered, and evaporated to a smaller fraction, which was poured into MeOH (1 L). The suspension was filtered to give the polymer, which was washed with methanol and dried in a vacuum oven. Polymer **35** was purified by preparative SEC.

**Poly{4,7-bis(4'-(2-ethylhexyl)-2,2'-dithiophene)benzo[1,2,5]-thiadiazole} (20):** yield 74%.  $^1\text{H}$  NMR (250 MHz,  $\text{CDCl}_3$ ):  $\delta$  = 8.22–7.77 (m, 1H), 7.16–6.93 (m, 2H), 6.84–6.27 (m, 1H), 2.87–2.21 (m, 2H), 1.82–1.53 (m, 2H), 1.43–1.02 (m, 16H), 1.02–0.84 (m, 12H). UV–vis ( $\text{CHCl}_3$ , nm): 428, 586 ( $\log \epsilon$  4.46, 4.53). SEC (500 Å + 10 000 Å + 1 000 000 Å)  $M_w$  = 86 362;  $M_p$  = 60 258;  $M_w/M_n$  = 1.994.

**Acknowledgment.** We gratefully acknowledge Lene Hubert for assistance with the ESCA measurements and Zheshen Li for technical support at the ASTRID storage ring and at the beamline. This work was supported by the Danish Technical Research Council (STVF 2058-03-0016) and the Danish Strategic Research Council (DSF 2104-04-0030, DSF 2104-05-0052).

**Supporting Information Available:** Detailed synthesis attempts of compounds **6**, **8**, and **9** and synthesis of polymers **14**–**16** with 2-ethylhexyl side chains, polymers **17**–**19** with hexyl side chains in a head-to-tail coupling, and polymer **20** with hexyl or dodecyl side chains; SEC traces of polymers **14**–**20** and UPS schemes of polymers **14**, **15**, **16**, and **20**; dedoping experiments of the polymers **16**, **18**, and **19** using hydrazine and ammonia; emission spectrum for polymer **18**. This information is available free of charge via the Internet at <http://pubs.acs.org>.

## References and Notes

- (1) (a) Andersson, M. R.; Thomas, O.; Mammo, W.; Svensson, M.; Theander, M.; Inganäs, O. *J. Mater. Chem.* **1999**, *9*, 1933–1940. (b) Brabec, C. J.; Sariciftci, N. S.; Hummelen, J. C. *Adv. Funct. Mater.* **2001**, *11*, 15–26. (c) Spanggaard, H.; Krebs, F. C. *Sol. Energy Mater. Sol. Cells* **2004**, *83*, 125–146. (d) Coakly, K. M.; McHehee, M. D. *Chem. Mater.* **2004**, *16*, 4533–4542. (e) Hoppe, H.; Sariciftci, N. S. *J. Mater. Res.* **2004**, *19*, 1924–1945. (f) Special Issue: The Development of Organic and Polymer Photovoltaics. *Sol. Energy Mater. Sol. Cells* **2004**, *83*, issues 2–3. (g) Special Issue: Organic-Based Photovoltaics. *MRS Bull.* **2005**, *30*, issue 1. (h) Krebs, F. C.; Spanggaard, H. *Chem. Mater.* **2005**, *17*, 5235–5237. (i) Li, G.; Shrotriya, V.; Huang, J.; Yao, Y.; Moriarty, T.; Emery, K.; Yang, Y. *Nat. Mater.* **2005**, *4*, 864–868.
- (2) Brabec, C. J.; Winder, C.; Sariciftci, N. S.; Hummelen, J. C.; Dhanabalan, A.; van Hal, P. A.; Janssen, R. A. J. *Adv. Funct. Mater.* **2002**, *12*, 709–712.
- (3) Dhanabalan, A.; van Duren, J. K. J.; van Hal, P. A.; van Dogen, J. L. J.; Janssen, R. A. J. *Adv. Funct. Mater.* **2001**, *11*, 255–262.
- (4) van Duren, J. K. J.; Dhanabalan, A.; van Hal, P. A.; Janssen, R. A. J. *Synth. Met.* **2001**, *121*, 1587–1588.
- (5) Winder, C.; Sariciftci, N. S. *J. Mater. Chem.* **2004**, *14*, 1077–1086.
- (6) Kiebooms, R. H. L.; Goto, H.; Akagi, K. *Macromolecules* **2001**, *34*, 7989–7998.
- (7) Wudl, F.; Kobayashi, M.; Heeger, A. J. *J. Org. Chem.* **1984**, *49*, 3382–3384.
- (8) Roncali, J. *Chem. Rev.* **1997**, *97*, 173–205.
- (9) McCullough, R. D. *Adv. Mater.* **1998**, *10*, 93–116.
- (10) Schouten, P. G.; Van Der Pol, J. F.; Zwikker, J. W.; Drenth, W.; Picken, S. J. *Mol. Cryst. Liq. Cryst.* **1991**, *195*, 291–305.
- (11) Van Pharm, C. *Synth. Commun.* **1986**, *16*, 689–695.
- (12) Krebs, F. C.; Spanggaard, H. *Sol. Energy Mater. Sol. Cells* **2005**, *88*, 363–375.
- (13) Hou, Q.; Xu, Y.; Yang, W.; Yuan, M.; Peng, J.; Cao, Y. *J. Mater. Chem.* **2002**, *10*, 2887–2892.
- (14) Pilgram, K.; Zupan, M.; Skiles, R. J. *Heterocycl. Chem.* **1970**, *7*, 629–633.
- (15) Karikomi, M.; Kitamura, C.; Tanaka, S.; Yamashita, Y. *J. Am. Chem. Soc.* **1995**, *117*, 6791–6792.
- (16) Kitamura, C.; Tanaka, S.; Yamashita, Y. *Chem. Mater.* **1996**, *8*, 570–578.
- (17) Bundgaard, E.; Krebs, F. C. *Polym. Bull.* **2005**, *55*, 157–164.
- (18) Nielsen, K. T.; Bechgaard, K.; Krebs, F. C. *Macromolecules* **2005**, *38*, 658–659.
- (19) Salzner, U.; Lagowski, J. B.; Pickup, P. G.; Poirier, R. A. *Synth. Met.* **1998**, *96*, 177–189.
- (20) Krebs, F. C. *Polym. Bull.* **2004**, *52*, 49–56.
- (21) Salaneck, W. R.; Lögdlund, M.; Fahlman, M.; Greczynski, G.; Kugler, T. *Mater. Sci. Eng.* **2001**, *R34*, 121–146.
- (22) Seki, K.; Furuyama, T.; Kawasumi, T.-O.; Sakurai, Y.; Ishii, H.; Kajikawa, K.; Ouchi, Y.; Masuda, T. *J. Phys. Chem. B* **1997**, *101*, 9165–9169.
- (23) Krebs, F. C.; Jørgensen, M. *Macromolecules* **2004**, *37*, 3958.
- (24) Krebs, F. C.; Jørgensen, M. *Macromolecules* **2002**, *35*, 7200–7206.
- (25) Jørgensen, M.; Krebs, F. C. *Pol. Bull.* **2003**, *51*, 23–30.
- (26) Lupsac, N.-O.; Catellani, M.; Luzzati, S. *Mol. Cryst. Liq. Cryst. Sci. Technol., Sect. A* **2002**, *385*, 121–128.

MA052683E